Topics in Catalysis (2022) 65:1700–1705
https://doi.org/10.1007/s11244-022-01612-7

ORIGINAL PAPER

Enhancement of Organic Solar Cells Through Macroscopic and Microscopic Models

Mahmoud N. Zidan[1] · Tawfik Ismail[2,3] · Sally S. Kassem[1,4] · Hayam G. Wahdan[4] · Irene S. Fahim[1]

Accepted: 30 March 2022 / Published online: 22 April 2022

Abstract

Organic solar cells performance enhancement is driven by improvements in device parameters. Compared to conventional silicon-based devices, the photo-generation process in organic devices is more complicated. This work investigates the possibility of improving the device performance theoretically by inserting microscopic parameters such as mobility, recombination factor, generation rate, and carriers density into the macroscopic single diode model. A proper selection of parameters leads to enhancement in (V_{oc}, I_{sc}) and (FF) while others should be avoided. A compromise between accuracy and speed can be achieved. Balanced mobility enhances short circuit current and the open-circuit voltage while higher values of ideality factor inhibit device performance.

Graphical Abstract

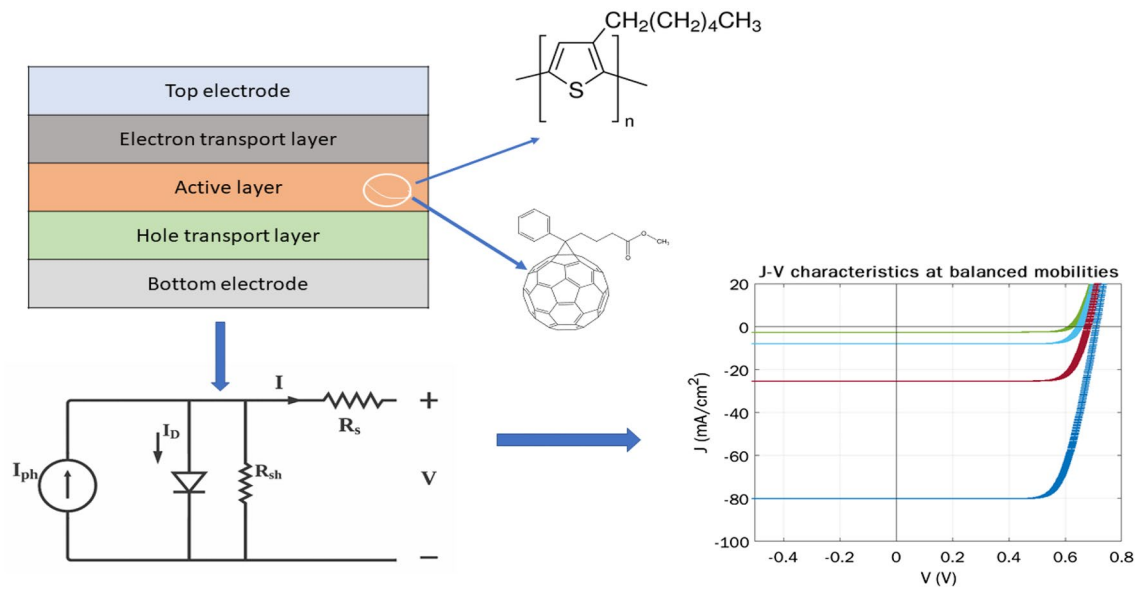

Keywords Organic solar cells · Device parameters · Macroscopic and microscopic models · Optimization

1 Introduction

Organic solar cells are a promising technology for electrical energy generation from sunlight due to it is low cost, fast production, flexibility, and already existing production technologies [1, 2]. Over the last two decades, significant

✉ Irene S. Fahim
isamy@nu.edu.eg

Extended author information available on the last page of the article

progress in the field has been made over different aspects of the technology in order to enhance device efficiency and stability. Researchers tackled the devices in a variety of ways, including manufacturing new materials, introducing different structures, developing experimental procedures for measuring device parameters, and building theoretical models for the faster study of the device [3–5]. Organic solar cells can be used in different fields due to their properties, which makes them more suitable than silicon-based devices. Based on the transparent properties of organic devices, it can be used in fields like agriculture applications allowing for sunlight to pass to plants and another portion for energy generation for higher productivity and farm monitoring[6]. The flexibility advantage made it easy for organic solar cells in indoor and outdoor applications in which area and fixation of devices was a major problem. It can be printed on clothes for human sensing applications and implanted with IoT devices in remote areas [7–9].

In the literature, many theoretical studies have been conducted to evaluate the possible enhancements of organic devices. In [10], an investigation of the effect of an interfacial layer such as ZnO on device parameters such as resistance and short circuit current has been carried out. Several works have evaluated the effect of active layer thickness on power conversion efficiency, including [11–13]. According to [14], optimization of an organic solar cell based on P3HT:ICBA for indoor applications had been accomplished by addressing device structure at varying illumination intensities. In [15], a hybrid theoretical and experimental technique for quantifying distinct recombination types with carrier lifetime was presented, which combined theoretical and experimental techniques. In the last few years, more techniques are being deployed in the field for the sake of rapid enhancement and device understanding. Machine learning algorithms are used for the selection of suitable organic materials as an active layer minimizing the time of experimental and extended search periods [16]. They were considering the examples of reported work that had been provided. As a result, the need for fast theoretical investigations has become essential for the development process.

The main contribution of this work is to explore the performance of various active materials theoretically by combining the simple diode model as a macroscopic model and the microscopic parameters of the organic solar cell such as mobility, recombination, and generation rates. The optimal macroscopic parameters of different devices, such as short circuit current density (J_{sc}), open-circuit voltage (V_{oc}), and fill factor (FF) will be optimized first, and then they will be mapped to a lower level in order to optimize the microscopic parameters. The results can be taken to the device design level, allowing for more rapid and cost-effective development. In Sect. 2 a brief description of the model is introduced. Section 3, represents the methodology while Sects. 4 and 5 represents results and the conclusion.

2 Modeling

The single diode model is among the most straightforward models that could be used to analyze solar cells in general. In this model, the solar cell is modeled as a current source connected in parallel with a diode and additional shunt resistance to accommodate the losses. This model is useful for exploring the overall behavior before the fabrication process, which provides fast design iterations and investigates the device's current-voltage characteristics. The model can establish the link between experimental measurements and theoretical results using parameters extraction [17–20]. Considering that the process of charge generation and collection in organic solar cells differs from that of silicon solar cells, the use of such models should be carried out carefully. The single diode model can be considered a composition consisting of three current components, each representing a microscopic process in the photovoltaic process. Considering the single diode model can be thought of as a composition of three current components [21].

$$J = J_0\left[\exp\frac{q(V - JR_s)}{nk_BT} - 1\right] + \frac{V - JR_s}{R_{sh}} - J_{ph} \tag{1}$$

where J_{ph} the photo-generated current density, n is the ideality factor of a diode, R_s represents the series resistance, R_{sh} is the shunt resistance, k_B is Boltzmann's constant, T is the operating temperature and q is the elementary charge. J_0 is the saturation current density which can be expressed as follows

$$J_0 = qk_r n_i^{\beta} d \tag{2}$$

where k_r is the recombination factor and n_i is the intrinsic carriers density [22].

Equation 1 is considered as a behavioral model of the solar cell. The behavioral model is particularly beneficial when evaluating the performance from the upper level in terms of performance parameters without going in details to the microscopic parameters when accuracy is not the primary concern compared to speed. They are widely employed by applications required to develop and implement a specific functionality within a limited time. Instead, physical models are more realistic in representing the device's physics, but they take longer to simulate a single structure run. Physical models are simplified by behavioral models, which map the physical parameters from the microscopic to the macroscopic level. The components of the single diode model are characterized by a range of physical parameters. The

main objective is to maximize the values that will support the required functionality. The photovoltaic process begins with the generation of charge carriers. It is necessary to accomplish this process depending on various parameters, including illumination, charge carrier mobility, and active layer thickness, to maximize the output current density. A model for J_{ph} has been developed in [23], which is given by

$$J_{ph} = \frac{-1 + \sqrt{1 + 4Gq\left(\frac{\mu_n+\mu_p}{\epsilon_0\epsilon_r\mu_n\mu_p}\right)\left(\frac{L_n^2L_p^2}{V_nV_p}\right)}}{\left(\frac{\mu_n+\mu_p}{\epsilon_0\epsilon_r\mu_n\mu_p}\right)\frac{2d}{V}\left(\frac{V_n}{L_n^2}+\frac{V_p}{L_p^2}\right)}, \tag{3}$$

where μ_n is the electron mobility, μ_p is the hole mobility G is the generation rate, L_n, L_p is electron and hole diffusion length, d is the active layer thickness, ϵ_0 is the permittivity of free space, ϵ_r is the relative permittivity of the active material and V is the applied voltage. While $\frac{\mu_n+\mu_p}{\mu_n\mu_p}$ is the effective mobility.

Equation (3) has been driven based on the following assumptions

(a) Illumination of the sample is uniform,
(b) Electrodes are non-injecting,
(c) Trapped carriers cannot be de-trapped by light excitons or free carriers,
(d) There is no exciton-exciton interactions,
(e) The excitonic injection of charge does not occur at the electrodes.

Recombination processes limit the transportation of generated charge carriers to their corresponding electrodes. In the single diode model, the diode ideality factor n and the saturation current density J_0 are the parameters representing the recombination process in the solar cell. Several types of recombination can occur within the device, including direct, Shockley-Read-Hall, and Auger recombination. Depending on the reaction order (β), each type has a corresponding value for the ideality factor that can be calculated by

$$n = \frac{2}{\beta} \tag{4}$$

For direct recombination $\beta = 2$, Shockely–Read–Hall recombination $\beta = 1$ and Auger recombination $\beta = 3$.

3 Methodology

The overall performance of the solar cell is determined by several factors, namely: short circuit current,open circuit voltage, parasitic resistances and fill factor. To obtain best performance, it is desired to have high efficiency, high fill factor, low series resistance and high shunt resistance. A solar cell is considered a multi-layer device with each layer contributing differently to the performance. These layers include the active layer, the front electrode and the back electrode. Thickness and type of material of these three layers has a direct impact on the efficiency, fill factor, and parasitic resistances [24–26]. To get the maximum performance of a solar cell, the efficiency and fill factor should be high, while the resistances should be low. The value of resistance arises from the processing of the device and material properties. It is controllable through different experimental ways. The device resistance has been related to mobility of charge carriers, device area and charge carriers concentration [27]. For the sake of fast solution effect of mobility is considered as the main contributing factor as its effect is common with different parameters. Along with carriers mobility ideality factor effect has been investigated as well.

Matlab is used to solve the $I-V$ equation by substituting equations 4 and 2 in Eq. 1. The thickness of the active layer is assumed to be greater than the diffusion length of holes and electrons. Diffusion length is assumed to be equal for both carriers.

$$d \geq l_n + l_p$$
$$\frac{L_p}{d} = \frac{L_n}{d} = 0.5$$

Different materials were used for this study. In Table 1, given the collection of active layers alongside with the measured parameters collected from experimental data in literature. Ranges around these values are used in this work. Our way of studying the performance is to change single parameter each time, starting by mobility then ideality factor and its related parameters and the generation rate a the end.

Optimization of the performance is a multi-parameter iterative problem. An iterative approach is used to maximize the performance by maximizing the photo-generated current while minimizing the other two current components given by Eq. 1.

Table 1 Numerical parameters of different organic active materials

Material	μ_e ($cm^2\ V^{-1}\ s^{-1}$)	μ_h ($cm^2\ V^{-1}\ s^{-1}$)	ϵ_r	References
Genaric organic	10^{-4}–10^{-7}	10^{-4}–10^{-7}	3.8	[22]
PT5DPP-PCBM	7.5×10^{-4}	3.5×10^{-4}	6.51	[28]
P3HT:PCBM	$10^{-4} - 10^{-8}$	$10^{-4} - 10^{-8}$	3.5	[23]
TQ1:PCBM	2×10^{-4}	2×10^{-4}	4	[29]
PBDB-T/ITIC-OE	1.2×10^{-5}	3.5×10^{-5}	6.1	[30]
CuPc-C60	7×10^{-4}	7×10^{-4}	3.5	[31]

4 Results and Discussion

The effect of mobility along with ideality factor and the generation rate will be introduced in the following subsections, with a dedicated subsection for each parameter representing its effect on device performance.

4.1 Mobility

Performance of the device, identified by J_{sc} and FF is calculated based on $J-V$ data in response to change in mobility. In first set of trials, hole mobility is fixed and electron mobility is changed. In second set, both are changed from trial to trial but they are equal. In first case $\mu_h = 1 \times 10^{-3}$ cm^2 V^{-1} s^{-1} while μ_e is changed in the range (1×10^{-4}–1×10^{-7} cm^2 V^{-1} s^{-1}). The maximum short circuit current density was found at $\mu_e = \times 10^{-7}$ cm^2 V^{-1} s^{-1} at which the photo-generated current is the same as the short circuit current, indicating that the generation and collection of carriers happen at maximum efficiency. At $\mu_e = \times 10^{-4}$ cm^2 V^{-1} s^{-1} a mismatch between J_{ph} and J_{sc} is found. It is noticed also that the change in both current densities is not significant. The maximum difference between two trials is $\approx$ 0.007. Table 2 represents the values of short circuit current, photo-generation current and fill factor at the condition of non-equal mobilities.The fill factor is constant for the device at different mobilities which indicates that the unbalanced mobilities does not affect the fill factor. Figure 1 represents the J–V relation at unbalanced charge carrier mobilities.

In case of equal mobilities the change in current densities is significant from case to case. The maximum short circuit current is obtained at $\mu_n = \mu_h = 10^{-7}$ cm^2 V^{-1} s^{-1}. The behavior of the device at this value is deviated from the behavior of the diode, it is closer to the behavior of a resistance. It is advised to go for different mobility to maintain the device physics. I-V and P-V characteristics of the device at different mobilities is shown in Fig. 2

Table 2 Device performance at unequal mobilities

μ_e	μ_h	J_{sc} (mA cm^{-2})	J_{ph} (mA cm^{-2})	FF
10^{-4}	10^{-3}	1.081	1.082	0.82
10^{-5}	10^{-3}	1.129	1.1297	0.82
10^{-6}	10^{-3}	1.134	1.134	0.82
10^{-7}	10^{-3}	1.134	1.134	0.82

4.2 Ideality Factor

Ideality factor affects the performance as well. The value of the ideality factor determines the short circuit current. In this study, the ideality factor has been changed from $n = 1$–2 at active layer thickness of $d = 100$–30 nm. The relation between the ideality factor and the short circuit current shows that the effect of the ideality factor is significant under certain threshold and above this limit the contribution becomes less significant as the J_{sc}–n curve saturates at higher values of n close to $n = 2$. For the same device parameters, different ideality factors of the device affects the V_{oc} which indicated by Fig. 3.

4.3 Generation Rate

Generation rate G is defined as the number of generated electrons in the device due to absorption of incident light. It is dependent on the device thickness. In this study, it has been used as a constant value over the device thickness. It contributes significantly to the device parameters like J_{sc} as higher G results in higher J_{sc}. Parameters such as ideality factor is expected to inhibit it is effect due to recombination.

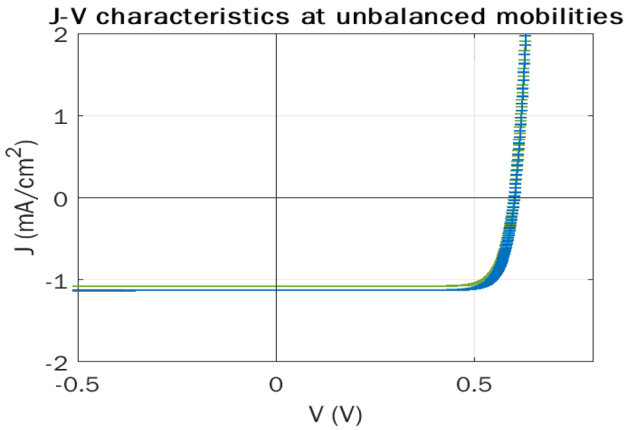

Fig. 1 J–V characteristics of solar cell with unbalanced mobilities

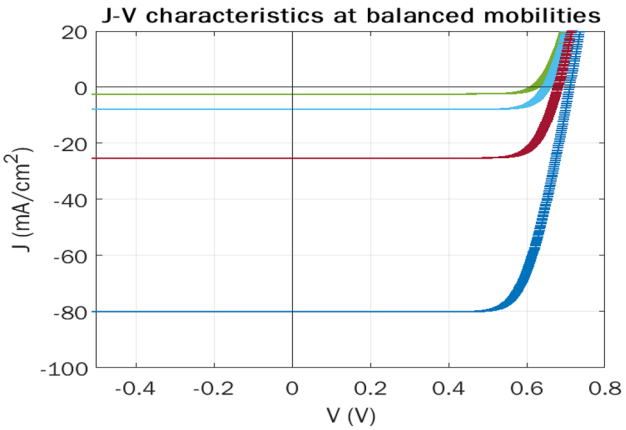

Fig. 2 J–V characteristics of solar cell with balanced mobilities

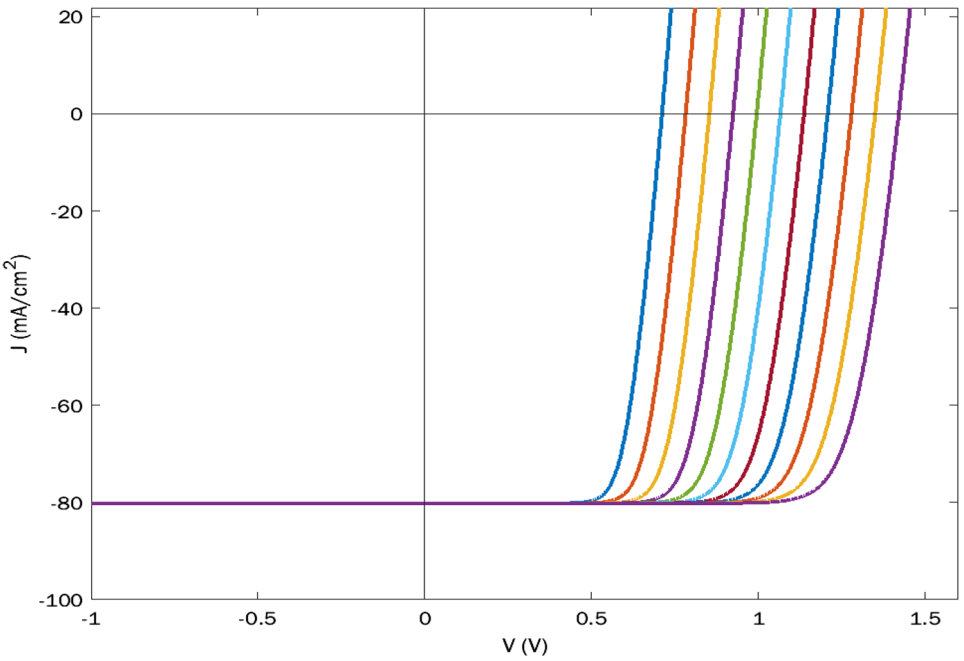

Fig. 3 J–V characteristics of solar cell with balanced mobilities

5 Conclusion

This work show the effect of different parameters on organic solar cells through combination of single diode model by doing several iteration on different parameters such as charge carriers mobility which results in a significantly low performance when the balance between hole and electron mobilities does not exist. Balanced mobilities shows superior performance than the unbalanced one. A theoretical maximum short circuit current can be obtained at $\mu_h = \mu_e = 1 \times 10^{-7}$ cm^2 V^{-1} s^{-1}. Also, the contribution of ideality factor to the device current shows a significant contribution at lower values of n while the device saturates at values near $n = 2$. The introduced work can be used as a prefabrication step to get organic solar cells targeting specific applications. Tuning of different parameters can affect transparency, conductivity, and flexibility to include organic solar cells in energy harvesting applications and sensing devices.

Funding Open access funding provided by The Science, Technology & Innovation Funding Authority (STDF) in cooperation with The Egyptian Knowledge Bank (EKB).

References

1. Riede M, Spoltore D, Leo K (2021) Organic solar cells—the path to commercial success. Adv Energy Mater 11(1):2002653
2. Ghosekar IC, Patil GC (2021) Review on performance analysis of P3HT:PCBM-based bulk heterojunction organic solar cells. Semiconduct Sci Technol 36(4):045005
3. Ma L, Zhang S, Zhu J, Wang J, Ren J, Zhang J, Hou J (2021) Completely non-fused electron acceptor with 3D-interpenetrated crystalline structure enables efficient and stable organic solar cell. Nat Commun 12(1):1–12
4. Xu X, Yu L, Peng Q (2021) Recent advances in wide bandgap polymer donors and their applications in organic solar cells. Chin J Chem 39(2):243–254
5. Sadoogi N, Rostami A, Faridpak B, Farrokhifar M (2021) Performance analysis of organic solar cells: opto-electrical modeling and simulation. Eng Sci Technol 24(1):229–235
6. Zhao Y, Zhu Y, Cheng H-W, Zheng R, Meng D, Yang Y (2021) A review on semitransparent solar cells for agricultural application. Mater Today Energy 22:100852
7. Fukuda K, Yu K, Someya T (2020) The future of flexible organic solar cells. Adv Energy Mater 10(25):2000765
8. Kim S, Jahandar M, Jeong JH, Lim DC (2019) Recent progress in solar cell technology for low-light indoor applications. Curr Altern Energy 3(1):3–17
9. Park S, Ahn H, Kim J-Y, Park JB, Kim J, Im SH, Son HJ (2019) High-performance and stable nonfullerene acceptor-based organic solar cells for indoor to outdoor light. ACS Energy Lett 5(1):170–179
10. Chen Z, Wang J, Jin H, Yang J, Bao Q, Ma Z, Tress W, Tang Z (2021) An underestimated photoactive area in organic solar cells based on a zno interlayer. J Mater Chem C9:11753–11760

11. dos Santos Rosa EH, Kowalski EL, Toledo LFRB (2021) Simulation of organic solar cells's power conversion efficiency. Sol Energy 221:483–487
12. Zidan MN, Ismail T, Fahim IS (2021) Effect of thickness and temperature on flexible organic P3HT:PCBM solar cell performance. Mater Res Express 8(9):095508
13. Li S, Hamada F, Nishikubo R, Saeki A (2022) Quantifying the optimal thickness in polymer: fullerene solar cells from the analysis of charge transport dynamics and photoabsorption. Sustain Energy Fuels 6:756
14. Vincent P, Shin S-C, Goo JS, You Y-J, Cho B, Lee S, Lee D-W, Kwon SR, Chung K-B, Lee J-J et al (2018) Indoor-type photovoltaics with organic solar cells through optimal design. Dyes Pigments 159:306–313
15. Schopp N, Brus VV, Lee J, Bazan GC, Nguyen T-Q (2021) A simple approach for unraveling optoelectronic processes in organic solar cells under short-circuit conditions. Adv Energy Mater 11(1):2002760
16. Mahmood A, Wang J-L (2021) Machine learning for high performance organic solar cells: current scenario and future prospects. Energy Environ Sci 14(1):90–105
17. Rasheed M, Alabdali O, Hassan HH et al (2021) Parameters extraction of a single-diode model of photovoltaic cell using false position iterative method. J Phys Conf Ser 1879:032113
18. Piliougine M, Guejia-Burbano R, Petrone G, Sánchez-Pacheco F, Mora-López L, Sidrach-de-Cardona M (2021) Parameters extraction of single diode model for degraded photovoltaic modules. Renew Energy 164:674–686
19. Song Z, Fang K, Sun X, Liang Y, Lin W, Xu C, Huang G, Yu F (2021) An effective method to accurately extract the parameters of single diode model of solar cells. Nanomaterials 11(10):2615
20. Cheknane A, Hilal HS, Djeffal F, Benyoucef B, Charles J-P (2008) An equivalent circuit approach to organic solar cell modelling. Microelectron J 39(10):1173–1180
21. Chan DS, Phang JC (1987) Analytical methods for the extraction of solar-cell single-and double-diode model parameters from iv characteristics. IEEE Trans Electron Devices 34(2):286–293
22. Würfel U, Neher D, Spies A, Albrecht S (2015) Impact of charge transport on current–voltage characteristics and power-conversion efficiency of organic solar cells. Nat Commun 6(1):1–9
23. Wilken S, Sandberg OJ, Scheunemann D, Österbacka R (2020) Watching space charge build up in an organic solar cell. Sol RRL 4(3):1900505
24. Nam YM, Huh J, Jo WH (2010) Optimization of thickness and morphology of active layer for high performance of bulk-heterojunction organic solar cells. Sol Energy Mater Sol Cells 94(6):1118–1124
25. Zang Y, Xin Q, Zhao J, Lin J (2018) Effect of active layer thickness on the performance of polymer solar cells based on a highly efficient donor material of PTB7-TH. The J Phys Chem C 122(29):16532–16539
26. Page ZA, Liu Y, Duzhko VV, Russell TP, Emrick T (2014) Fulleropyrrolidine interlayers: tailoring electrodes to raise organic solar cell efficiency. Science 346(6208):441–444
27. Servaites JD, Yeganeh S, Marks TJ, Ratner MA (2010) Efficiency enhancement in organic photovoltaic cells: consequences of optimizing series resistance. Adv Funct Mater 20(1):97–104
28. Neukom MT, Züfle S, Ruhstaller B (2012) Reliable extraction of organic solar cell parameters by combining steady-state and transient techniques. Org Electron 13(12):2910–2916
29. Shoaee S, Stolterfoht M, Neher D (2018) The role of mobility on charge generation, recombination, and extraction in polymer-based solar cells. Adv Energy Mater 8(28):1703355
30. Nithya K, Sudheer K (2020) Numerical modelling of non-fullerene organic solar cell with high dielectric constant itic-oe acceptor. J Phys Commun 4(2):025012
31. Yang F, Forrest SR (2008) Photocurrent generation in nanostructured organic solar cells. ACS Nano 2(5):1022–1032

Authors and Affiliations

Mahmoud N. Zidan[1] · Tawfik Ismail[2,3] · Sally S. Kassem[1,4] · Hayam G. Wahdan[4] · Irene S. Fahim[1]

Mahmoud N. Zidan
m.nazih@nu.edu.eg

Tawfik Ismail
tismail@cu.edu.eg

Sally S. Kassem
s.kassem@fci-cu.edu.eg

Hayam G. Wahdan
hayam@fci-cu.edu.eg

[1] Smart Engineering Systems Center (SESC), Nile University, Giza 12677, Egypt

[2] National Institute of Laser Enhanced Sciences, Cairo University, Giza 12677, Egypt

[3] Wireless Intelligent Networks Center (WINC), Nile University, Giza 12677, Egypt

[4] Faculty of Computers and Artificial Intelligence, Cairo University, Giza 12613, Egypt